Performance Analysis of Microstrip Antenna with Semi-eliptical Slotted Patch and Defected Ground Structure at 28 GHz for 5G Communication Systems

Ayane Lebeta Goshu, Mulugeta Tegegn Gemeda, and Kinde Anlay Fante(✉)

Faculty of Electrical and Computer Engineering, Jimma Institute of Technology, Jimma University, PO Box 378, Jimma, Ethiopia
{ayane.goshu,mulugeta.geneda,kinde.anlay}@ju.edu.et

Abstract. The fifth-generation (5G) wireless communication networks are required to support ultra-high speed broadband communications. The utilization of millimeter wave (mm-wave) bands is needed to meet these requirements. However, communication in the mm-wave band has different propagation properties such as relatively high path losses and atmospheric absorption; the signals are easily blocked by the obstacle and low diffraction around the objects. It is crucial to design compact size antennas with high gain and bandwidth to mitigate these effects. In this paper, a semi-elliptical slotted microstrip patch antenna with defected ground structure configuration operating in the millimeter waveband is proposed. The antenna is designed using Rogers RT5880 substrate material with a thickness of 0.34490 mm and a dielectric constant of 2.2 to operate at 28 GHz. The semi-elliptical slotted radiating patch is mainly used to improve bandwidth and radiation efficiency. The defected-ground structure is used to enhance both the bandwidth and gain of the antenna. The defect structure (slot) positions and sizes are optimized to obtain considerably high bandwidth and gain. The inset-fed input matching network becomes easy due to introducing semi-elliptical slots in the radiating patch and defected ground structure. The overall structure of the antenna has a size of ($5.8 \times 6.4 \times 0.3449$) mm. The proposed microstrip patch antenna (MPA) with a defect structure is simulated using CST-MW studio and found that its return loss, bandwidth, and gain are –37.784 dB, 1.132 GHz, 7.128 dBi; whereas a typical rectangular MPA without defect structure achieves –34.189 dB, 0.978 GHz, 6.67 dBi, respectively. The simulation results show that simultaneously introducing defected structures in the patch and ground plane of the proposed MPA significantly influences its performance. As compared to existing works, the proposed antenna shows significantly improved performance. It shows a suitable characteristic, in terms of size, bandwidth, and gain, for the needs of IoT applications offered by 5G technology.

Keywords: Bandwidth · Gain · Etched structure · Fifth-generation (5G) · Microstrip patch antenna

M. L. Berihun (Ed.): ICAST 2021, LNICST 411, pp. 304–317, 2022.
https://doi.org/10.1007/978-3-030-93709-6_20

1 Introduction

In the current 5G and future 6G systems, a large number of mobile devices are expected to be connected to the current cellular networks, which increase data traffic and system connections, resulting in the need for massive resources in the upcoming years [1, 2]. One of the promising technologies for meeting these system requirements is the use of millimeter-wave frequency band, and the fifth-generation of wireless technology is rolling out and has already been launched in some parts of developed countries [3]. In 5G communication systems, the mm-wave frequency band, which can provide unauthorized bandwidth of up to 1 GHz and low latency, is considered a key factor in resolving exponential data traffic increment. Thus, by using the mm-wave frequency band, the 5G system supports three major usage scenarios. These are enhanced high-speed movable and fixed broadband, low latency communications, and machine to machine (M2M) communications [4].

The first usage scenario is the key characteristic of this platform, particularly in the early stage of its deployment. Thus, the productivity and efficiency of device connectivity in society will be improved by the 5G infrastructure's superiority over existing cellular networks. The second one offers a minimal delay, in which several end-users within the range of the same base station can use up to 1Gbps internet connection for low latency applications such as drone control and unrestricted call rates. In the last usage scenario, a large number of links from low-power machines can be assisted by 5G technology. In this technology, the supported data rate will reach a up to one hundred times the bandwidth of the 4G networks. Thus, for instantaneous connectivity, 5G frameworks and advancements migrate to advanced mobile networks, allow large machine-type interactions, and encourage network applications that demand ultra-high reliability and minimal latency [5, 6].

To achieve the 5G wireless communication systems' anticipated performances, three frequency bands are considered: low, medium, and high-frequency bands. However, the selection of a band relies on its characteristics, precisely the capacity of spectrum resources and radio signal propagation. Accordingly, under 3GPP release 15, two new frequency bands have been defined for 5G communication systems. These are frequency band one (450 MHz–6 GHz, in which the upper limit can be extended up to 7.125 GHz) and frequency band two (24.25 GHz–52.6 GHz). Recently, the initial deployment of 5G communication systems has been launched in China, South Korea, and Japan using the first frequency band as the working frequency. However, in order to meet the demands of different applications, primarily for fixed/mobile 5G applications that need significant bandwidth to support higher speeds (greater than 1.0 Gbps) with lower latency, the FCC approved the reallocation of wide bandwidths of more than one GHz at 28, 37, and 39 GHz [5, 7].

Thus, for the next phase deployment of indoor broadband access point applications, introducing fixed point-to-point and point-to-multipoint high-speed backhaul connectivity at home, and mid-sized cell outdoor applications, the 28 GHz frequency band has got high research interest from the scientific research community. This frequency band contains large bandwidth and provides the opportunity of assigning bulky spectrum resources. The size of the antenna at this frequency band is very compact; therefore, the antenna designer can integrate a large number of array elements to construct massive antenna arrays, which can be easily integrated into tiny IoT devices.

Moreover, the 28 GHz band could be made available by reallocating the local multipoint block distribution service, which is suitable for various applications. Mobile applications, which are currently a core aspect of 5G deployment endorsed by national carriers and other organizations, may use the 28 GHz band [8, 9]. More specifically, the complete deployment of a 5G scheme needs antenna infrastructure planning and the introduction of new technological resolutions, which can be more reliable to build inside the public service buildings such as train stations, stadiums, and shopping malls. Antennas for 5G wireless technology at a higher frequency are expected to be wideband to achieve high-speed connectivity [10].

In applications where a strong connection with low latency is needed, an antenna with a high gain is required to mitigate the radio wave impediment, such as human beings, which are likely barriers to the mm-wave system, causing more significant transmission loss due to high operating frequency [11]. In general, wireless technology advancements require less weight, low cost, easy for mass manufacturing, compatible with planar and non-planar surfaces, and mechanically stable while mounted on rigid surfaces [12]. Microstrip patch antennas are one of the proposed solutions and are considered a good option in this regard. They are ideal for spacecraft, satellites, aircraft, vehicles, and lightweight, portable communication types of equipment. The MPA, therefore, continues to play a vital role in the fastest-growing field of wireless communication [13, 14].

However, compared to traditional microwave antennas, MPA has some drawbacks. The substrate thickness affects the antenna bandwidth and radiation efficiency by increasing surface waves and spurious feed radiation of the feeding lines. Consequently, undesired cross-polarized radiation is caused by feed radiation effects. The MPA also experiences losses such as dielectric, conductor, and radiation losses resulting in bandwidth and gain reduction. These pose a design challenge for the MPA designers to meet the broadband and high gain requirement of 5G mm-wave communication systems [15–18].

With an aim to overcome the limitations of MPA and enhance its performance for 5G systems, several research studies have been carried out in [3, 9, 11, 19–29]. These studies have employed various approaches, including a U-slotted patch [3], adding extra structure on radiating patch [11], modifying the feeding techniques [19, 20], the defected ground structure and Y-shaped patch [21], X-shape slotted [22], introducing multiple slots [23, 24], etched patch [25], various substrate material types [26], a substrate integrated waveguide patch [27]. The antenna designs in [9, 11, 20, 26, 28, 31] show high gain and directivity from reported simulation results. High radiation efficiency is achieved in [26], and a wide bandwidth antenna is reported in [9, 32]. However, the magnitude of VSWR of antennas reported in these studies is large.

Likewise, works in [11, 20, 28, 29] achieved narrow bandwidth. Therefore, to improve the bandwidth, various MPA designs appeared in [21–25] and achieved wide bandwidth. Nevertheless, low gain and large magnitude of return loss and VSWR are achieved in [21, 22] because of their inefficient impedance matching. The radiation efficiency of the antennas in [9, 21, 24, 29] is low. Antenna with significantly improved radiation efficiency was proposed in [11, 22, 25, 26]. Lastly, a good performance in gain, directivity, and VSWR is achieved [3, 21, 24].

To sum up, the performance of existing single-element MPA reported in recent scientific literature reveals that the bandwidth is narrow, gain and directivity of the radiation pattern are low to be used in the 5G wireless communication systems. The existing patch antenna studies show no single antenna with good performance in all key performance metrics. Therefore, the scientific research community has continued its effort to boost the performance of MPA in terms of all performance metrics.

This study's main focus is to enhance the bandwidth and gain of single element rectangular MPA for 5G communication systems. Defect structure is introduced in both the patch and the ground plane, and also, the antenna key physical dimensions are tuned to enhance these performance parameters. The remaining sections of this paper are presented as follows. Section 2 discusses the design specification and the proposed microstrip patch antenna. In Sect. 3, the simulation result analysis and discussions are revealed. Lastly, Sect. 4 presents the conclusion and remarks of the study.

2 Materials and Methods

The basic procedure of patch antenna design starts with \selecting the resonant frequency and substrate material type with its thickness and dielectric constant. Next, by substituting the selected four initial design parameters in the governing equation given in [17, 31], all the remaining preliminary physical dimensions of the antenna such as width and length of the patch, ground plane, microstrip feeder line, and feed point of the antenna are determined. Design parameters and fundamental governing equation used to calculate MPA dimension are given in Table 1 [5, 17, 31].

Table 1. Design parameters and fundamental governing equations.

Designed parameters	Symbols	Governing equations
Substrate thickness	SH	$\mathrm{SH} = \frac{0.3\mathrm{C}}{2\pi \mathrm{F}o\sqrt{\varepsilon r}}$
Patch width	PW	$\mathrm{PW} = \frac{\mathrm{C}}{2\mathrm{Fo}\sqrt{\frac{\varepsilon r+1}{2}}}$
Patch length	PL	$\mathrm{PL} = PL_{eff} - 2\Delta PL$
Length microstrip transmission line	LMTL	$\mathrm{LMTL} = \frac{\lambda 0}{4\sqrt{\varepsilon \mathrm{r}}}$
Width of microstrip transmission line	WMTL	$\mathrm{WMF} = \frac{\frac{{}_{5.98}\mathrm{SH}\frac{1}{\exp\left(\mathrm{ZMHF}_{\sqrt{\varepsilon_r+1.41}}\right)} - \mathrm{t}}{87}}{0.8}$
Inset length	IL	$\mathrm{I}L = \left(\frac{\mathrm{PL}}{\pi}\right)\mathrm{Cos}^{-1}\left(\sqrt{\frac{\mathrm{Z_O}}{\mathrm{Z_L}}}\right)$
Ground plane width	GPW	GPW = PW + 6SH
Ground plane length	GPL	GPL = PL + 6SH

Where C denotes the speed of light (3×10^8 m/s), Fo is the operating frequency (28 GHz).

Accordingly, in this study, Rogers RT5880 substrate material with a thickness of 0.3449 mm and a dielectric constant of 2.2 is selected. A 28 GHz is chosen as a resonant frequency. Therefore, using these initial design parameters, all physical dimensions of substrate thickness, length, and width of the radiating patch, feeder-line, inset and ground plane, and feed point location can be calculated using the equations given in Table 1. After obtaining the preliminary dimensions of the patch antenna, the dimensions are tuned to optimize its performance using the CST Microwave Studio simulator. Table 2 shows the initially calculated and optimized dimensions of the rectangular microstrip patch antenna.

To enhance the performance of the rectangular MPA in terms of directivity, bandwidth, and gain, different shapes of defect structures can be incorporated in the radiating patch or/and the ground plane. After optimizing the rectangular MPA, a semi-elliptical slot is introduced to both the radiating element and group plane of rectangular MPA. This half-ellipse part on both the radiating element portion and the ground plane has been etched out to boost some of the performance characteristics, indicated in Fig. 1.

Table 2. Initial calculated and tuned dimension of typical and modified MPA.

Design parameters	Typical MPA		Semi-elliptical Slotted MPA	
	Calculated values (mm)	Optimized values (mm)	Calculated values (mm)	Optimized values (mm)
PW	4.23519	4.7	4.23519	4.73
PL	3.40451	3.3398	3.40451	3.66
LMTL	1.80589	1.861	1.80589	1.67
WMTL	0.82137	0.821	0.82137	0.8
IL	0.89268	0.89268	0.89268	1
IW	0.02475	0.3	0.02475	0.2
GPW	6.30459	6.4	6.30459	7
GPL	5.47391	5.8	5.47391	7

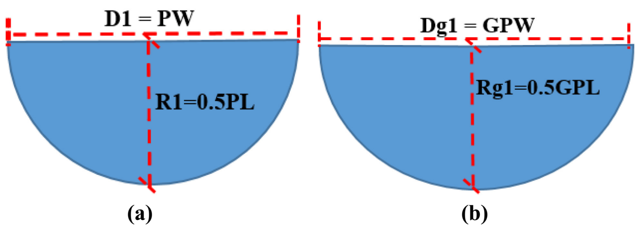

Fig. 1. The defected structure on the patch (a) and ground plane (b).

The defect structure dimension is half-ellipse with the diameter of the major axis is equal to the patch width for the radiating element (D1 = PW) and ground plane width for the ground plane part (Dg1 = GPW). Similarly, the diameter of the minor axis equal to the patch length for the radiating element (R1 = 0.5PL) and ground plane length for the ground plane part (Rg1 = 0.5 GPL) as shown in Fig. 1. The complete physical structures of the proposed rectangular and modified semi-elliptical slotted MPA are shown in Fig. 2. After setting the dimensions of the slot, CST Microwave Studio simulator is used to determine the optimal dimensions of the slots. The optimal performance of the antenna is obtained when the diameter of the major axis of the slot is 3.15 mm for radiating element and 4.67 mm for the ground plane structure; and when the diameter of minor axis of the slot is 1.22 mm for the radiating element and 2.33 mm for the ground plane structure. Inset-fed structure is used to improve the reflection coefficient of the antenna.

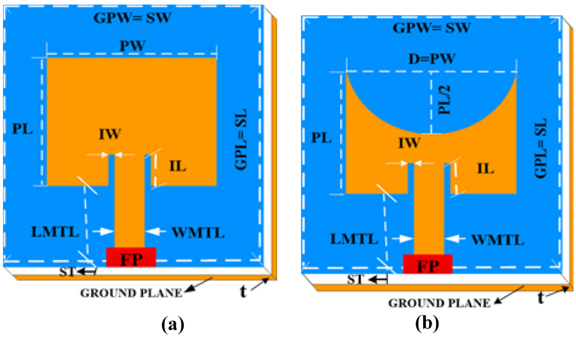

Fig. 2. (a) Typical rectangular MPA and (b) Semi-elliptical slotted MPA.

3 Simulation Result Analysis and Discussions

In this section, simulation-based performance analysis of MPA with a different configuration for 5G communication systems is discussed. The performance of MPA structures shown in Fig. 3 is compared. Frequency-domain solver of the CST Microwave Studio simulator has been used to analyze the performance of these antenna structures in terms of S-parameter plot (return loss), bandwidth, radiation efficiency, VSWR, gain, and directivity of the radiation pattern. As described in Sect. 2, the design of the proposed antenna started with rectangular MPA with an inset-feed structure, as shown in Fig. 2 (a). A semi-elliptical slot is introduced in the ground plane in Fig. 3 (a). Then, a semi-elliptical structure is introduced in the radiating patch of the antenna, as shown in Fig. 3 (c). In a similar pattern, we have introduced semi-elliptical slots of different sizes, as shown in Fig. 3 (d–f).

The impact of introducing different structures in MPA is studied, and comparative analysis is performed. Figure 3 (a–c) shows the effect of introducing defect structures on the performance of the microstrip patch antenna. The simulated reflection coefficients of the three structures are shown in Fig. 4. Among the three structures, the structure without defect (Fig. 3a) has achieved the lowest reflection coefficient, bandwidth, directivity, gain, and radiation efficiency. Introducing a semi-elliptical slot on the ground structure (Fig. 3b) improves the bandwidth, gain and directivity of the antenna. The semi-elliptical slot on the radiating patch of the antenna (Fig. 3c) improves the bandwidth and radiation efficiency, as indicated in Table 3.

Further study was conducted to analyze the effect of the size of the slot on the performance of the MPA. The size of the semi-elliptical slot is varied as shown in Fig. 3 (d–f) and its effect is analyzed as depicted in Fig. 5. The performance of the optimized antenna structure (Fig. 3 (e)) achieves the best performance among all the other structure as depicted in Fig. 5. Making the slot size above or below the optimal dimension of the antenna, deteriorates the performance of the antenna.

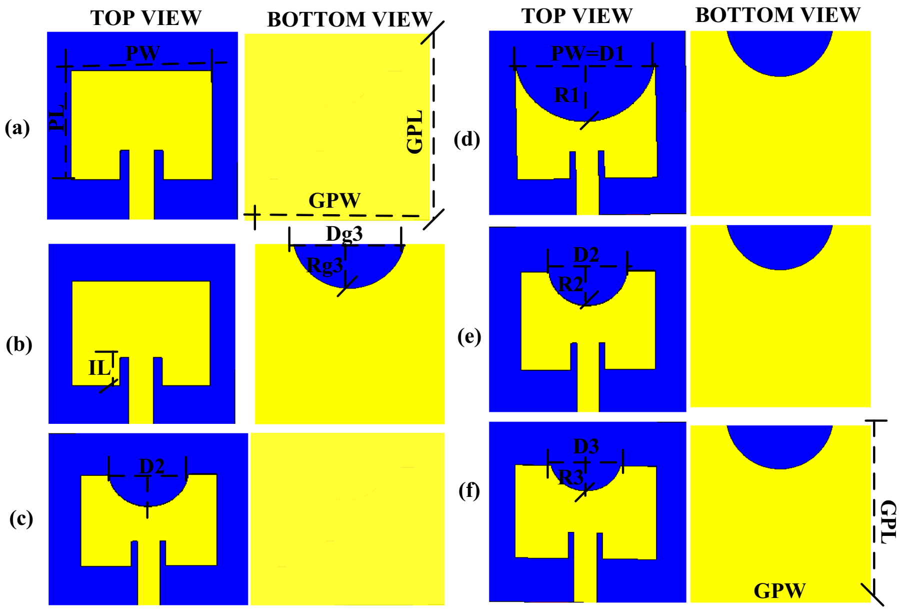

Fig. 3. Physical structure of examined MPA: (a) Typical MPA, (b) Typical MPA with DGS, (c) Defected patch with Typical Ground Plane, and (d, e, f) varying patch defect dimension size with DGS with D1 = PW, R1 = 0.5PL, D2 = 2 * PW/3, R2 = PL/3, D3 = PW/2, R3 = PL/4, and Rg3 = 2 * GPL/3, Dg3 = GPW/3.

The simulated results reveal that the analyzed regular and semi-elliptical slotted MPA's return loss is less than -10dB between 27.522 GHz and 28.5 GHz, as shown in Fig. 6a and between 27.419 GHz and 28.551 GHz as shown in Fig. 6b, respectively. At the operating frequency (28 GHz), the return losses are –34.189dB and –37.784dB, respectively. Therefore, as can be seen from these results, the optimized semi-elliptical slotted MPA achieved minimum return loss compared to the other structures.

In addition, from Table 4, it is evident that the return loss of the proposed antenna is lower than the simulation results achieved in [3, 5, 9, 11, 18, 20, 22, 24, 26, 28–30]. However, it is large as compared to the results of antenna designs reported in [19, 23, 25, 31, 32]. Furthermore, the –10dB bandwidth of the proposed antenna is 1.132 GHz

(4.043%) as shown in Table 3. The obtained bandwidth of modified antenna is wide as compared to the previous similar works reported in [9, 11, 18–20, 26, 29–32] as listed in Table 4. Conversely, achieved bandwidth is narrow compared to designs demonstrated in [3, 5, 22–25].

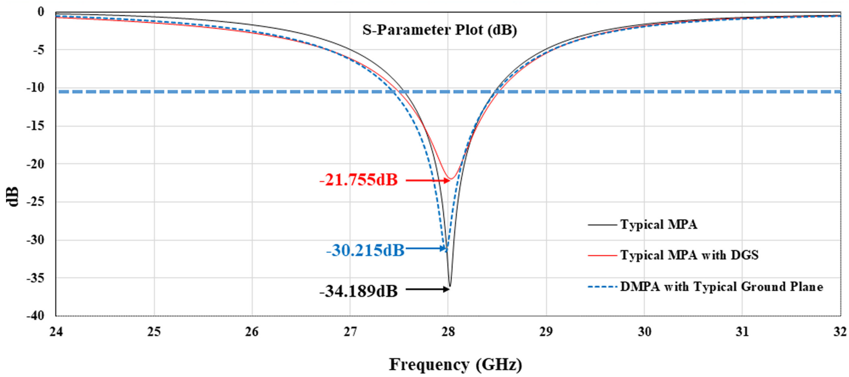

Fig. 4. The simulation results of the reflection coefficients (S_{11}) of the structures shown in Fig. 3 (a–c).

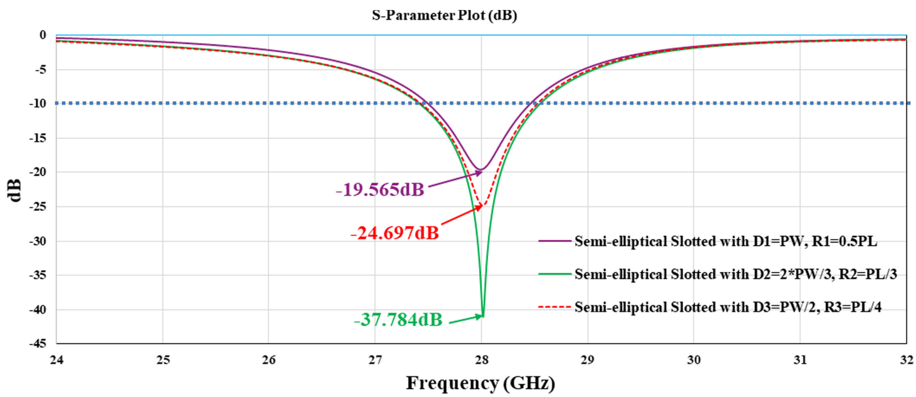

Fig. 5. Simulation results of the reflection coefficients of the antenna structures shown in Fig. 3 (d–f).

Generally, the minimum return loss and wide bandwidth have been attained since poor impedance matching at the feeder point, and patch edge has been minimized using the inset-feed impedance matching technique and tuning the design parameters. Besides, by creating the defect on both the patch antenna and ground plane and the fringing patch width, which is used to change the current distribution of both structures, the high input impedance at the resonant frequency is minimized. Accordingly, considerable input power is transferred to the transmission line, and small input power is returned as a return loss. Thereby, the antenna's radiation efficiency is increased, which leads to enhanced bandwidth.

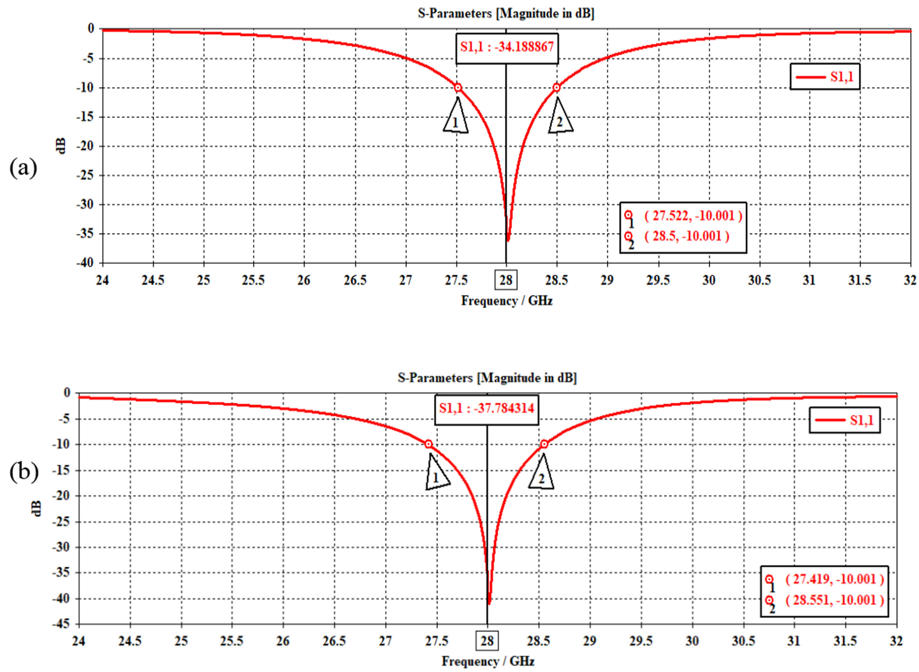

Fig. 6. Return loss plot of typical (a) and modified (b) single MPA.

Table 3. Comparison of the performance of different MPA structures.

Antenna structures (Fig. 3)	Performance metrics					
	S_{11} (dB)	BW (GHz)	G (dBi)	D (dBi)	VSWR	η*tot*(%)
(a)	–34.189	0.978	6.667	6.689	1.039	98.22
(b)	–21.755	1.092	7.038	7.121	1.178	98.37
(c)	–30.215	1.117	6.931	6.942	1.064	99.66
(d)	–19.565	0.959	7.112	7.174	1.235	97.49
(e)	–37.784	1.132	7.128	7.183	1.026	98.74
(f)	–24.697	1.085	7.094	7.132	1.124	98.79

The VSWR plot of the proposed modified single rectangular MPA is shown in Fig. 7. As observed from the plot, at the resonant frequency, the VSWR of the modified single rectangular MPA is 1.026. In a rigorous way of description, as the feeder-line is moved to the patch's center, the impedance mismatch between the patch's transmission line and the edge will be reduced [17]. In this study, the patch and ground plane's introduced defect highly influences input impedance at the resonant frequency (Fig. 7).

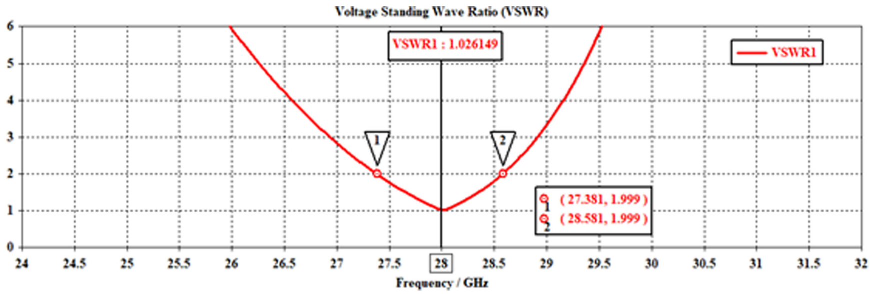

Fig. 7. VSWR plot of the optimized MPA with semi-elliptical slotted patch and DGS.

Also, the patch width, the inset length, and the inset gap have been carefully tuned, and then the impedance mismatch between the feeder line of the microstrip and the patch edge becomes a matched point, i.e., the input power is passed to the patch with lower standing waves of voltage. Consequently, maximum power is transferred to the radiating patch. Compared to the design reported in [9, 18, 20, 22, 26, 28–30], the optimized MPA has achieved a minimum magnitude of VSWR.

Figure 8 shows the 3D radiation pattern of the proposed optimized MPA. As displayed in Fig. 8, the MPA gain is 7.128 dBi, and the achieved directivity of the antenna is 7.183 dBi. As shown in Table 4, the gain of the proposed antenna outperforms the reported designs of [5, 9, 18, 22, 23, 25, 29, 30]. But, it is low as compared with simulation results given in [3, 19, 20, 26, 31, 32].

The improved radiation pattern directivity is achieved as compared to designs demonstrated in [22, 28]. Nevertheless, it is lower than the directivity of antenna designs in [11, 30]. Besides, the radiation efficiency and total radiation efficiency of the proposed antenna structure are –0.05442 dB (98.75%) and –0.05513 dB (98.74%), respectively, which is higher than antennas cited in [9, 11, 25, 26, 29–32].

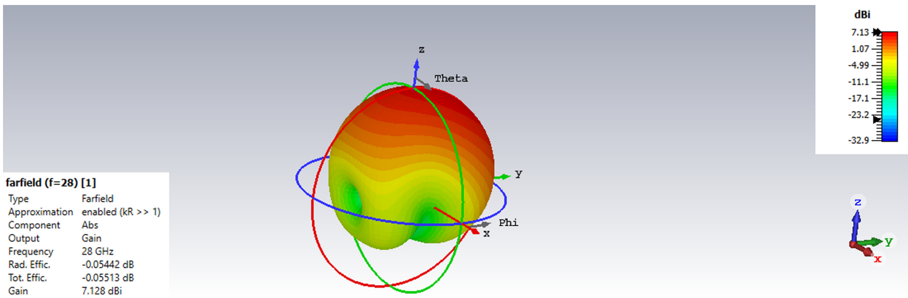

Fig. 8. 3D radiation pattern of the proposed typical (a) and modified (b) single MPA.

Generally, in this study, the proposed single element rectangular MPA has attained better and improved results in terms of directivity, radiation efficiency, and gain.

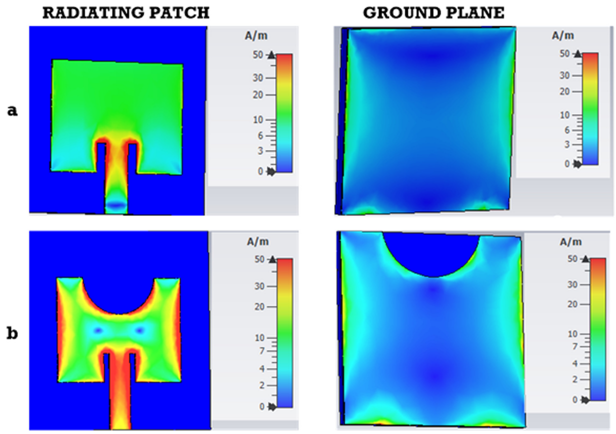

Fig. 9. Current distributions of typical (a) and semi-elliptical slotted (b) rectangular MPA.

As shown in Fig. 9, simultaneously introducing defect structure on patch and ground plane significantly alters the current distributions of both structures and then increases the radiatixon efficiency of the antenna. Besides, good impedance matching has been made in the middle of the edge of the patch and the microstrip transmission line. The dimensions of key design parameters have been tuned, which minimize the magnitude of the return loss, VSWR, and raise the radiation efficiency and bandwidth.

Table 4. Comparison of Reported Works and the Proposed Modified Single MPA.

Ref.	S_{11} (dB)	BW (GHz)	G (dBi)	D (dBi)	VSWR	η_{rad} (%)
[3]	–32	5.82	9.49	-	-	-
[5]	–22.51	5.57	3.6	-	-	-
[9]	–13.48	0.847	6.63	-	1.5376	70.18
[11]	–12	0.5	-	8.33	1.01	85.33
[18]	–14.15	0.8	6.0611	7.767	1.48784	-
[19]	–59.37	0.43	8.5	-	-	-
[20]	–34.05	0.582	8.00	-	1.75	-
[22]	–20.03	2.1	5.2	6.16	1.22	-
[23]	–48.25	4.07	5.61	-	-	-
[24]	–28.47	1.9	7.63	7.632	1.078	-
[25]	–39.37	2.46	6.37	-	1.022	86.73
[26]	–17.83	0.44	12.013	-	1.2994	92.655
[28]	–22.2	-	-	6.85	1.34	-
[29]	–27.7	0.463	6.72	-	1.22	75.87
[30]	–20.24	0.572	7.18	7.404	1.2156	94.95
[31]	–38.86	1.046	7.587	-	1.023	98.214
[32]	–54.492	1.062	7.55	-	1.011	98
This work	**–37.784**	**1.132**	**7.128**	**7.183**	**1.026**	**98.75**

Where S_{11} denotes return loss, BW denotes bandwidth, D denotes directivity, G is gain, VSWR denotes voltage standing wave ratio, and η_{rad} denotes radiation efficiency.

4 Conclusions

In this paper, bandwidth and gain enhancement of the single element rectangular MPA for 5G communication systems have been performed successfully. Simulation results of this study reveal that the bandwidth, return loss, gain, and radiation efficiency of the proposed modified single element MPA are 1.132 GHz (4.043%), –37.784 dB, 7.128 dBi, and (98.75%), correspondingly. As compared to designs reported in [11, 18–20, 26, 29, 30], and [31], in this study the bandwidth is increased by 632MHz, 332 MHz, 702 MHz, 550 MHz, 285 MHz, 669 MHz, 560 MHz, 86 MHz, respectively. Likewise, the gain has been boosted by 3.528 dBi, 0.98 dBi, 1.066 dBi, 1.928 dBi, 1.518 dBi, 0.758 dBi, as compared with the antenna design presented in [5, 9, 18, 22, 23], and [25], respectively.

Furthermore, the magnitude of the return loss is minimized by –15.584 dB, –24.304 dB, –25.78 dB, –23.63 dB, –17.754 dB, –19.95 dB, –15.584 dB, –17.544 dB, as compare to work presented in [5, 9, 11, 18, 22, 26, 28, 30], respectively. Lastly, as seen as simulation result reported in [9, 11, 25, 26, 29] the radiation efficiency has been increased by 28.5%, 13.42%, 12.02%, 6.095%, 22.9%, respectively. Therefore, in general, it can be concluded that by introducing etched structure on radiating element and ground plane structures and tuning the key design parameters simultaneously, the rectangular MPA's performance is greatly improved compared to other related works in terms of the bandwidth, gain, and radiation efficiency. The designed MPA provides highly competitive performance with a very compact size suitable for the emerging 5G communication systems.

References

1. Xiaoxiong, G.: A multilayer organic package with 64 dual-polarized antennas for 28 GHz 5G communication. In: Proceedings of the IEEE International Microwave Symposium, pp. 1899-1901. IEEE (2018)
2. Mungur, D., Duraikannan, S.: Microstrip patch antenna at 28 GHz for 5G applications. J. Sci. Technol. Eng. Manage. Adv. Res. Innov. **1**(1), 20–22 (2018)
3. Hussain, W.: Multiband microstrip patch antenna for 5G wireless communication. Int. J. Eng. Works **01**(01), 15–21 (2020). https://doi.org/10.34259/ijew.20.7011521
4. Sohail, A., Hamid, K., Khan, U., Muhammad, I., Nasir, S., Jamal, A.: Design and analysis of a novel patch antenna array for 5G and millimeter-wave applications. In: 2019 2nd International Conference on Computing, Mathematics and Engineering Technologies, IEEE, pp. 30–31, Sukkur, Pakistan (2019)
5. Przesmycki, R., Bugaj, M., Nowosielski, L.: Broadband microstrip antenna for 5G wireless systems operating at 28 GHz. Electronics **10**(1), 1 (2020). https://doi.org/10.3390/electronics10010001
6. Liu, Y., et al.: Non-Orthogonal Multiple Access for 5G and Beyond. In: Proceedings of the IEEE October 2017, pp. 1-33(2017)

7. Hakanoglu, B., Sen, O., Turkmen, M.: A square microstrip patch antenna with enhanced return loss through defected ground plane for 5G wireless networks. In: 2nd URSI AT-RASC, Gran Canaria, 28 May-1 June 2018
8. Zhang, J., Ge, X., Li, Q., Guizani, M., Zhang, Y.: 5G millimeter-wave antenna array: design and challenges. In: IEEE Wireless Communication, pp. 106-112 (2017)
9. Omar, D., Dominic, B., Onyango, K., Franklin, M.: A 28GHz rectangular microstrip patch antenna for 5G applications. Int. Res. Publ. House. J. Eng. Res. Technol. **12**(6), 854–857 (2019)
10. Ershadi, E., Keshtkar, A., Abdelrahman, A., Xin, H.: Wideband high gain antenna sub-array for 5G applications. Progr. Electromagn. Res. C **78**, 33–46 (2017)
11. Abdelsalam, M., Abdalla, M., Essam, H.: Design and analysis of millimeter-wave microstrip patch antenna for 5G applications. In: International Conference on Technical Sciences (ICTS2019), pp. 137-142, Tripoli, Libya (2019)
12. Sridevi, S., Mahendran, K.: Design of millimeter-wave microstrip patch antenna for MIMO communication. Int. Res. J. Eng. Technol. **4**(10), 1513–1518 (2017)
13. Shanthi, S., Jayasankar, T., Christydass, P., Venkatesh, P.: Wearable textile antenna for GPS application. Int. J. Sci. Technol. Res. **8**(11), 3788–3791 (2019)
14. Jones, S., Gunavathi, N.: Codirectional CSRR inspired printed antenna for locomotive short-range radar. In: ICICI (2017)
15. Johari, S., Jalil, M., Ibrahim, S., Mohammad, M., Hassan, N.: 28GHz Microstrip Patch Antennas for Future 5G. Malaysian. J. Eng. Sci. Res. **2**(4), 01–06 (2018). https://doi.org/10.26666/rmp.jesr.2018.4.1
16. Vamsi, N., Sravanthi, G., Narmada, K., Kavya, K., Swamy, G., Durgarao, M.: A microstrip patch antenna design at 28 GHz for 5G mobile phone applications. Int. J. Electron. Elect. Comput. Syst. **7**(3), 1–10 (2018)
17. Balanis, C.: Antenna Theory Analysis and Design, 3rd edn. John Wiley and Sons Inc, Hoboken, New Jersey (2005)
18. Kavitha, M., Kumar, T., Gayathri, A., Koushick, V.: 28 GHz printed antenna for 5G communication with improved gain using array. Int. J. Sci. Technol. Res. **9**(03), 5127–5133 (2020)
19. Jeyakumar, P., Chitraand, P., Christina, G.: Design and simulation of directive high gain microstrip array antenna for 5G cellular communication. Asian J. Appl. Sci. Technol. **2**(2), 301–313 (2018)
20. Chaitanya, N., Poornima, M., Prahelika, P., Monika, R., Rozy, T.: Inset feed compact millimeter-wave microstrip patch antenna at 28 GHz for future 5G applications. Int. Res. J. Eng. Technol. **06**(03), 3137–3141 (2019)
21. Wahaj, A., Abir, Z., Abdennaceur, B.: Patch antenna with improved performance using DGS for 28GHz applications. IEEE Access, International Conference on Wireless Technologies, Embedded and Intelligent Systems, Fez, Morocco, 3-4 April 2019
22. Gupta, V., Vijay, S., Gupta, P.: A Novel Design of Compact 28GHz Printed Wideband Antenna for 5G Applications. Int. J. Innov. Technol. Explor. Eng. **9**(3), 3936–3700 (2020)
23. Ghazaoui, Y., El Alami, A., El Ghzaoui, M., Das, S., Barad, D., Mohapatra, S.: Millimeter wave antenna with enhanced bandwidth for 5G wireless application. J. Instrum. **15**(01), T01003–T01003 (2020). https://doi.org/10.1088/1748-0221/15/01/T01003
24. Karthikeyan, V., Vignesh, S., Ayyavar Reddy, K., Bhargavi Reddy, G., Aparna Sekhar, R. S.: A millimeter wave based circular slot loaded microstrip patch antenna for 5G communication. IOP Conf. Ser. Mater. Sci. Eng. **590**(1), 012059 (2019). https://doi.org/10.1088/1757-899X/590/1/012059

25. kaeib, A.F., Shebani, N.M., Zarek, A.R.: Design and analysis of a slotted microstrip antenna for 5G communication networks at 28GHz. In: 19th International Conference on Sciences and Techniques of Automatic Control and Computer Engineering, March 24-26, 2019
26. Subramaniam, S., Selvaperumal, S., Jayapal, V.: High gain compact multi-band microstrip patch antenna for 5G network. Int. J. Adv. Sci. Technol. **29**(1), 1390–1410 (2020)
27. Mohamed, B., Hegazy, E.A.: Design and analysis of 28GHz rectangular microstrip antenna. WSEAS Trans. Commun. **17**, 2224–2864 (2018)
28. Sarade, S.S., Ruikar, S.D., Bhaldar, H.K.: Design of microstrip patch antenna for 5G application. In: Pawar, P.M., Ronge, B.P., Balasubramaniam, R., Vibhute, A.S., Apte, S.S. (eds.) Techno-Societal 2018, pp. 253–261. Springer, Cham (2020). https://doi.org/10.1007/978-3-030-16848-3_24
29. Darsono, M., Wijaya, A.R.: Design and simulation of a rectangular patch microstrip antenna for the frequency of 28 GHz in 5G technology. J. Phys. Conf. Ser. **1469**(1), 012107 (2020). https://doi.org/10.1088/1742-6596/1469/1/012107
30. Mulugeta, T.: Comparative performance assessment of different rectangular microstrip patch antenna array configurations at 28GHz for 5G wireless applications. Master's thesis, Jimma University, Jimma Institute of Technology, Jimma, Ethiopia (2020)
31. Gemeda, M.T., Fante, K.A., Goshu, H.L., Goshu, A.L.: Design and Analysis of a 28GHz microstrip patch antenna for 5G communication systems. Int. Res. J. Eng. Technol. **8**(02), 881–886 (2021)
32. Fante, K.A., Gemeda, M.T.: Broadband microstrip patch antenna at 28GHz for 5G wireless applications. Int. J. Elect. Comput. Eng. **11**(3), 2238–2244 (2021)